IEEE Photonics Journal
An IEEE Photonics Society Publication

Open Access

Temperature Sensor Based on Fiber Ring Laser With Cascaded Fiber Optic Sagnac Interferometers

Volume 13, Number 2, April 2021

Weihao Lin
Liyang Shao, *Senior Member, IEEE*
Yibin Liu
Sankhyabrata Bandyopadhyay
Yuhui Liu
Weijie Xu
Shuaiqi Liu
Jie Hu
Mang I Vai, *Senior Member, IEEE*

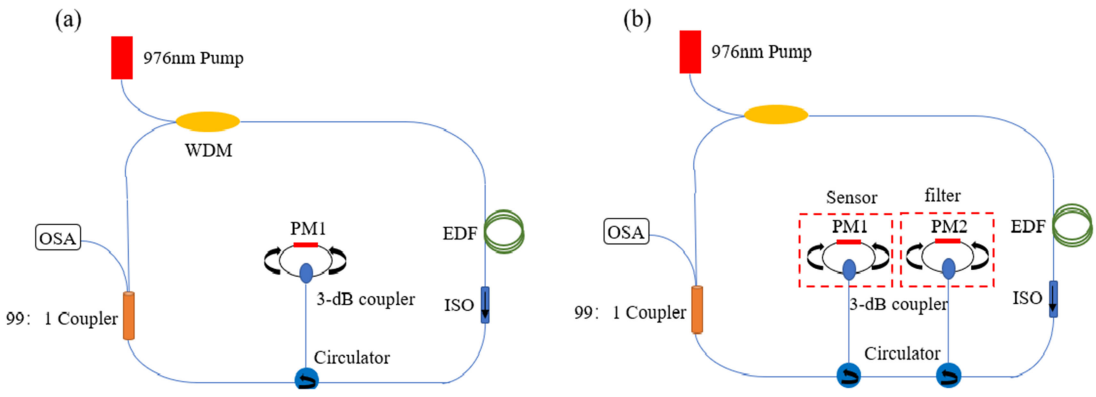

DOI: 10.1109/JPHOT.2021.3065567

Temperature Sensor Based on Fiber Ring Laser With Cascaded Fiber Optic Sagnac Interferometers

Weihao Lin,[1,2] **Liyang Shao**,[1] ***Senior Member, IEEE***, **Yibin Liu**,[1] **Sankhyabrata Bandyopadhyay**,[1] **Yuhui Liu**,[1] **Weijie Xu**,[1] **Shuaiqi Liu**,[1,2] **Jie Hu**,[1] **and Mang I Vai**,[2] ***Senior Member, IEEE***

[1]Department of Electrical and Electronic Engineering, Southern University of Science and Technology, Shenzhen 518055, China
[2]Department of Electrical and Computer Engineering, Faculty of Science and Technology, University of Macau, Macau 999078, China

DOI:10.1109/JPHOT.2021.3065567

Manuscript received December 16, 2020; revised March 2, 2021; accepted March 9, 2021. Date of publication March 11, 2021; date of current version April 7, 2021. This work was supported by the startup fund and Post-Doctoral research fund from the Southern University of Science and Technology and the Shenzhen government. Corresponding author: Liyang Shao (e-mail: shaoly@sustech.edu.cn).

Abstract: A new temperature fiber ring laser (FRL) sensor based on a cascaded Sagnac loops fiber structure is proposed and experimentally demonstrated. The optical FRL sensor consists of cascaded Sagnac loops by inserting two polarization-maintaining optical fibers (PMF) with slightly different lengths. PMF with length of 56 cm and 75 cm are used in Sagnac loops as a filter and sensing unit in laser cavity. The working principle of the sensor is based on the phase shift (θ) caused by birefringence between two principal polarization modes and enhance the sensitivity by constructing a Vernier-scale. In an appropriate temperature range (25 °C - 31 °C), the detection sensitivity of FRL sensor based on a cascaded Sagnac structure is significantly higher than other FRL sensors. Thanks to the laser sensing system, the sensitivity can be modulated by changing the free spectral range (FSR). The experimental results show that the temperature sensitivity of the cascade Sagnac structure sensor is - 4.031 nm / °C, which is five times higher than that of FRL sensor base on the single Sagnac structure.

Index Terms: Fiber ring laser, cascaded Sagnac loop, temperature sensors.

1. Introduction

In the last few decades, fiber-optic sensors have attracted extensive attentions in engineering and scientific applications. Due to the advantages of their compact size, high resolution, immunity to electromagnetic interference and cost-effective deployment of the sensors. Lots of traditional optical fiber sensor schemes have been proposed over the last twenty years. Temperature sensors are designed and fabricated based upon the principles of fiber Bragg grating (FBG) [1]–[3], Mach-Zehnder interferometer (MZI) [4]–[6], and Fabry-Perot interferometers (FPI) [7]–[9]. Recently, there is a growing interest in all-fiber laser sensors, since it has the advantages of high sensitivity, good stability, low insertion loss and high signal-to-noise ratio. In general, fiber laser sensors can be classified into three types: distributed Bragg reflector(DBR) fiber laser [10]–[12], distributed feedback(DFB) laser [13]–[15] and fiber ring laser(FRL) [16]. It was observed that the tunable erbium-doped based FRL is a good candidate for temperature sensing since its spectrum is

geared to the telecommunication wavelength window. Various FRL sensors have been extensively investigated to measure temperature [24]–[26], gas pressure [17], refractive index (RI) [18], strain [19], and curvature sensing [20]. Those sensors are useful in biomedicine, health monitoring, aviation, hydrostatic pressure [21]–[23], etc.

Contemplating the different sensing structures, performance enhancement of the sensitivity and stability of FRL temperature sensor is one of the research directions that has attracted extensive attention. A temperature FRL sensor based upon liquid filled photonic crystal fiber (PFC) with a sensitivity of -1.747 nm/ °C was proposed by Yang *et al.* [24]. However, liquid evaporation has a great influence on the stability of the sensor. Zhao *et al.* used a core-offset Mach-Zehnder (MZ) interferometer to measure the refractive index and temperature simultaneously, with a temperature sensitivity is 0.049 nm/ °C and a signal to noise ratio of 60dB [25]. An FPI is inserted into the FRL working as a temperature sensor through an optical fiber circulator [26]. The temperature sensitivity is 0.249 nm/ °C with a signal to noise ratio of 52dB. Over recent years, substantial research efforts have been devoted to the development of FRL sensor based on Sagnac interferometer [27]–[29]. A Sagnac loop structure FRL sensor with high temperature sensitivity of 1.739 nm/ °C, narrow 3-dB bandwidth of less than 0.05 nm, and high signal to noise ratio of 50 dB was proposed by Yao *et al.* [30]. The result shows that with the insertion of FBG, the temperature resolution has been improved to 10^{-6} °C [31]. However, limited by the intrinsic structure of the sensor, the temperature sensitivities obtained among these works are not high as traditional fiber sensors. Besides, cascaded interferometers can significantly enhance the spectral shift range through the Vernier effect. The use of cascaded interferometers as filters for interval-adjustable FRLs has been proposed in recent years [32]–[34]. However, to the best of our knowledge, FRL sensor operated under the principle of Vernier effect has not been widely proposed.

In this work, we proposed an ultra-high sensitivity FRL temperature sensor with cascaded Sagnac loops. Narrow 3-dB bandwidth less than ∼0.67 nm and a high signal to noise ratio of ∼30 dB is experimentally demonstrated. The theoretical model and experimental design of the proposed method are discussed in detail. The temperature sensitivity of the proposed sensor is about -4.031 nm/ °C, significantly higher than previously reported FRL based sensors [24]–[26]. The sensitivity enhances ∼5 times based on the Vernier effect in the cascaded Sagnac interferometers than single Sagnac loop. Unlike traditional cascaded Sagnac loops fiber sensor [35]. The FRL sensor is able to demodulate the wavelength change directly, relaxing the need for transmission spectra calculation procedure. The stability and measurement error of the proposed sensor is also analyzed experimentally. The proposed temperature sensor can be used for several engineering applications including biomedical science and aviation monitoring.

2. Principles

The schematic diagram of the cascaded Sagnac loop interferometer is shown in Fig. 1. The whole system is consisted of two 3 dB couplers and two PMF with similar length. In the Sagnac interferometer, two polarization states can be represented by Jones matrix. The transmission of the electric field is described by Jones vector [36]:

$$E_{in} = \begin{bmatrix} E_{in}^{x} \\ E_{in}^{y} \end{bmatrix} \tag{1}$$

where E_{in} is the input electric field. $E_{in}^{x}$and $E_{in}^{y}$are the two orthogonal polarization components of E_{in}. The Jones matrix of the 3dB coupler can be described as [36]:

$$\mathrm{T}_C = \begin{bmatrix} \sqrt{1-\kappa} & j\kappa \\ j\sqrt{\kappa} & \sqrt{1-\kappa} \end{bmatrix} \tag{2}$$

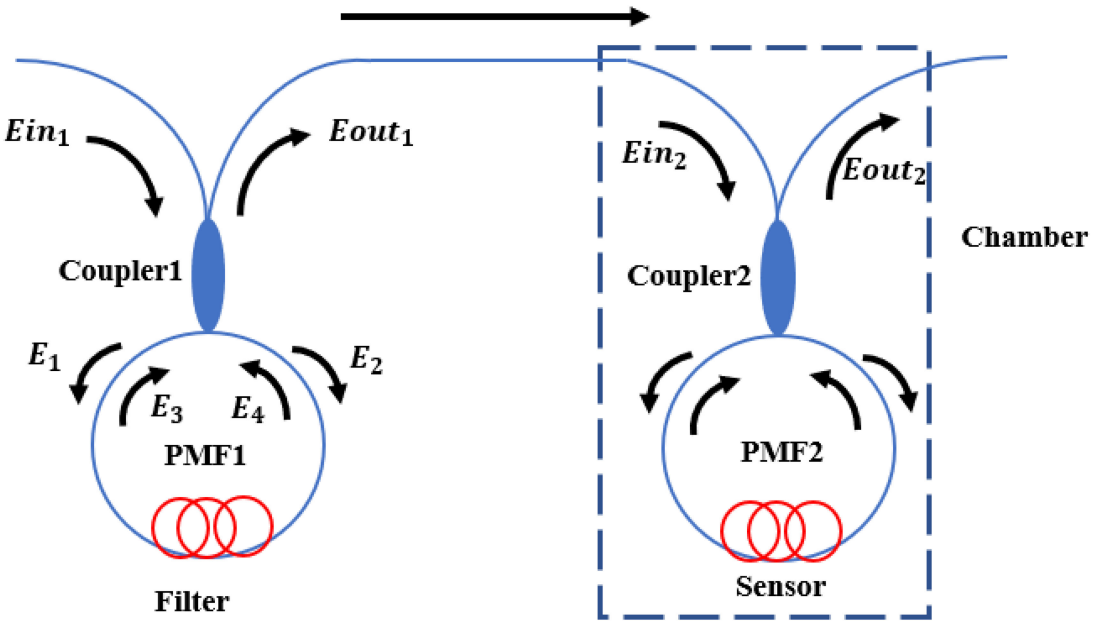

Fig. 1. Configuration of the proposed cascaded Sagnac loop sensors based on the Vernier effect.. PMF: polarization-maintaining fiber.

where κ is the coupling coefficient of the optical coupler. The output electric fields of the optical coupler are described as:

$$\begin{bmatrix} E_1 \\ E_2 \end{bmatrix} = T_C \begin{bmatrix} E_{in} \\ 0 \end{bmatrix} \tag{3}$$

where E_1 and E_2 represent the two output electric fields of the optical coupler, respectively. The Jones matrix of the PMF can be expressed as [36]:

$$T_{PMF} = \begin{bmatrix} e^{-j\varphi} & 0 \\ 0 & e^{j\varphi} \end{bmatrix} \tag{4}$$

$$\varphi = \frac{\pi L \Delta n}{\lambda} \tag{5}$$

where φ is the phase of the two orthogonal components of the electric field in the PMF, λ is the wavelength, Δn is the refractive index difference between the fast axis and the slow axis of the PMF. L is the length of the PMF. The output of the electric fields is denoted as E_3 and E_4 after propagating through PMF,which can be written as:

$$E_3 = \begin{bmatrix} e^{-j\varphi} & 0 \\ 0 & e^{j\varphi} \end{bmatrix} \begin{bmatrix} cos\theta & sin\theta \\ -sin\theta & cos\theta \end{bmatrix} E_1 \tag{6}$$

$$E_4 = \begin{bmatrix} cos\theta & -sin\theta \\ sin\theta & cos\theta \end{bmatrix} \begin{bmatrix} e^{-j\varphi} & 0 \\ 0 & e^{j\varphi} \end{bmatrix} E_2 \tag{7}$$

Here θ is the phase shift of light propagating through PMF between two polarization modes. After transmission through the loop the output electric field of the Sagnac interferometer can be calculated as:

$$E_{out} = j\sqrt{\kappa} E_3 + \sqrt{1-\kappa} E_4 \tag{8}$$

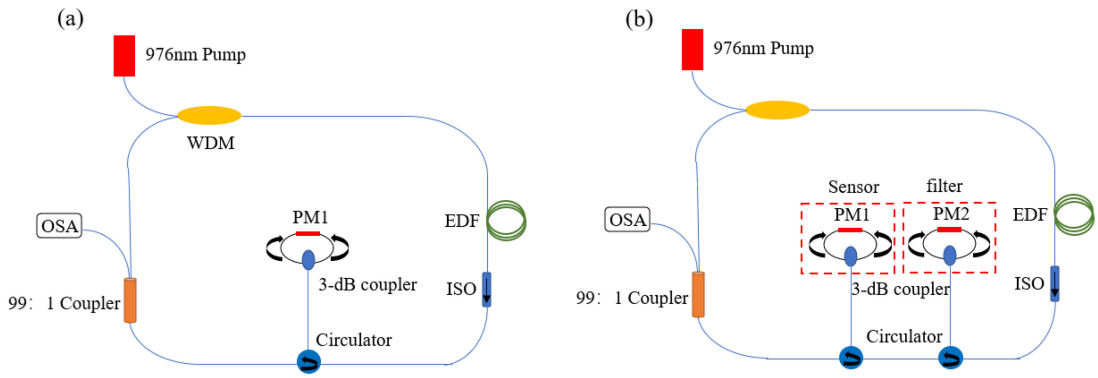

Fig. 2. (a)The intracavity temperature sensing system of the FRL with Sagnac loop (b) The intracavity temperature sensing system of the FRL with cascaded Sagnac loop. WDM: wavelength division multiplexer, ISO: optical isolator, EDF: Erbium-doped fiber, OSA: optical spectrum analyzer, PMF: polarization-maintaining fiber.

From Eqs.1–8, we can calculate the transmission spectra of a single Sagnac loop interferometer. The transmission spectra of a single Sagnac loop interferometer with different lengths of PMF is shown in Fig. 3. The lengths of PMF we used were 56 cm and 75 cm, respectively. The wavelength interval between two adjacent transmission peaks, named free spectral range (FSR) can be calculated by the following equation [35]:

$$FSR = \frac{\lambda^2}{BL} \tag{9}$$

where B is the birefringence of the PMF. When the temperature is changed by ΔT, a corresponding wavelength shift $\Delta\lambda$ will be introduced as [35]:

$$\Delta\lambda = S\lambda \tag{10}$$

where S is the temperature sensitivity of the proposed sensor. Thus, the real phase shift can be written as [36]:

$$\varphi = \frac{2\pi BL}{\lambda - S\Delta T} \tag{11}$$

The spectra of a single Sagnac interferometer under different PMF lengths is obtained in Fig. 3. According to eq. (8), PMF with length of 56 cm and 75 cm are inserted into the cascaded fiber ring, respectively. To improve the sensitivity of the temperature sensor. We constructing a Vernier-scale with two cascaded Sagnac interferometers. Vernier-scale is widely used in high-precision and short-distance ranging to enhance the accuracy of detection. It mainly uses the change of small measurement value to cause large-scale change of alignment graduation. Measure by overlapping two tick marks. The peak spacing of the spectrum is affected by the length of PMF, which produced different FSR. The Saganc loop of the sensing one in Fig. 1 shifts the wavelength without changing the FSR. The peak appears at the wavelength where two interference peaks overlap, and the height of each peak is determined by the overlap. The envelope period is given by [32]:

$$\frac{fsr_{sensor} * fsr_{filter}}{\left|fsr_{senosr} - fsr_{filter}\right|} \tag{12}$$

When the interference peaks of two independent Sagnac loops overlapping, the maximum peak wavelength appears in the cascaded loop. If the sensor loop shifts with temperature change, the

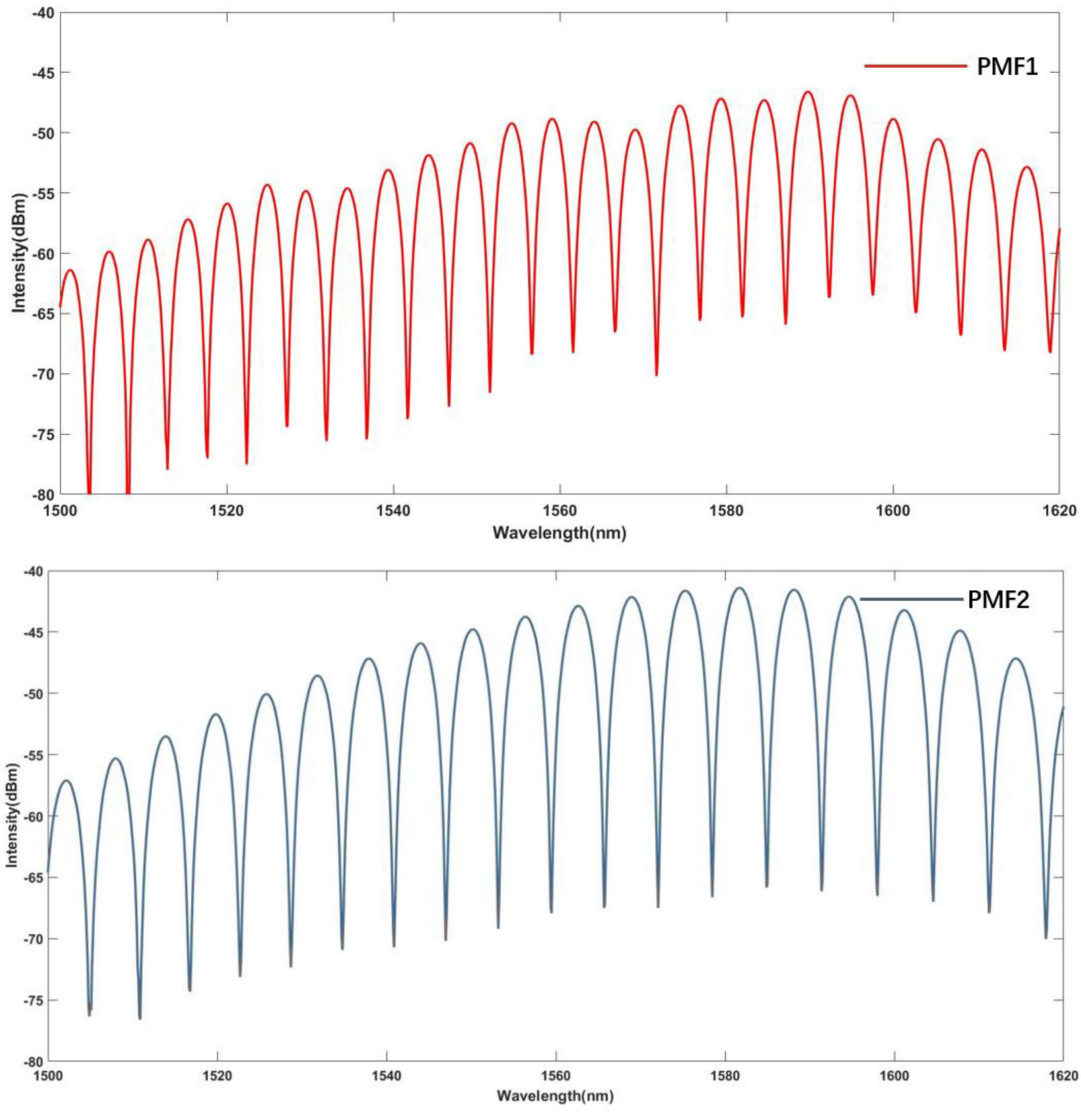

Fig. 3. The transmission spectra of the Sagnac loop interferometer with different PMF lengths. PMF1 = 0.56m, PMF2 = 0.75 m.

peak will be transmitted to the adjacent peak. The magnification is:

$$\frac{fsr_{filter}}{\left|fsr_{senosr} - fsr_{filter}\right|} \tag{13}$$

Fig. 1 shows how the Vernier-scale concept is applied to Sagnac loops. The interference signal of the first Sagnac loop is used as the input for the second sensing loop. The total transmission spectrum of cascaded Sagnac loops is the product of each Sagnac loop. The two interference peaks of each Sagnac loop are partially overlapped, and the height of each envelope will be determined by the overlap amount. In practical application, we can get the ideal FSR by controlling the length of PMF. The filter Sagnac ring is a good shield of the ambient temperature or strain changes, which is a fixed part of the Vernier scale. The second sensor Sagnac is more like the sliding part of the Vernier scale, because the change of temperature will cause the shift of the interference wavelength.

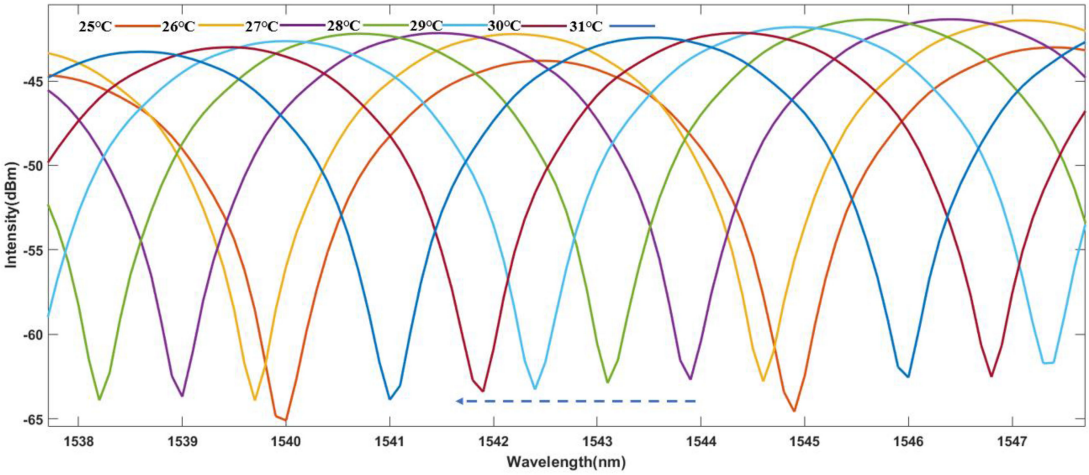

Fig. 4. The transmission spectrum shifts of single Sagnac interferometer with temperature change from 25 °C to 31 °C.

3. Experimental Details

In the cascaded loops system, the first Sagnac loop works as the reference part of the Vernier-scale, meanwhile also protecting the system from external interference. The second sensor is the sliding part of the Vernier-scale. As shown in Fig. 2. the experimental setup of the FRL sensor includes a laser pump source with a tunable output power from 150mW to 500mW, a wavelength division multiplexing (WDM), an isolator (ISO), two cascaded Sagnac loops and couplers. 1% of the output light energy was sent to OSA for analysis.

The pump light from a 980 nm laser source (PL-974-500-FC/APC-P-M) was launched into the FRL by a 980/1550 nm WDM. A section of 1.6m long EDF was adopted as the gain medium. Two PMFs (Changfei, PM 1550_125-18/250_Y) with lengths of 56 cm and 75 cm are used to construct Sagnac loop. The backscattered optical signal from the Sagnac loop was blocked by an optical isolator (PIIS1550DP01212) to prevent spatial hole-burning. Temperature change was applied by placing the sensing part of Sagnac loop inside a dry bath chamber. The output spectrum of the temperature sensing system is measured by an OSA (YOKOGAWA, AQ6370D) via a 1:99 coupler. The 1% output of the coupler is connected with OSA, and the other end is connected with WDM to couple the optical transmission back to the ring cavity. In this system, one Sagnac loop is used as a filter and the other working as a temperature sensor. The detection sensitivity is effectively enlarged by Vernier scale effect.

In order to verify the working principle of the sensor, a pre-experiment is carried out. By using supercontinuum light source. The spectral shifts of single Sagnac loop and cascade Sagnac loops were measured at different temperatures. The output transmission spectrum of the temperature sensor system composed of Sagnac loop is shown in Fig. 4. Besides, As shown in Fig. 5, the cascade Sagnac loop structure can significantly improve the detection sensitivity due to the Vernier effect. fsr_{senosr} and fsr_{filter} were measured to be 6.31 nm and 4.92 nm, respectively, as shown in Fig. 3. Therefore, the calculated enhancement factor is 4.54. The sensing characteristics of the single and cascaded Sagnac loops were tested by placing the sensor in a dry bath while the temperature was tuned from 25 °C to 31 °C. The interval between each measurement is half an hour. As shown in Fig. 5, there is only one dominant transmission peak two sidelobes. The sidelobe suppression ratio is about 10 dB, demonstrating excellent a single-wavelength stability ability by cascaded Sagnac interferometers.

The pre-experimental results show that the wavelength has a blue-shifted with the increase of temperature. In Fig. 6, the temperature sensitivity of Sagnac structure sensor and cascade Sagnac

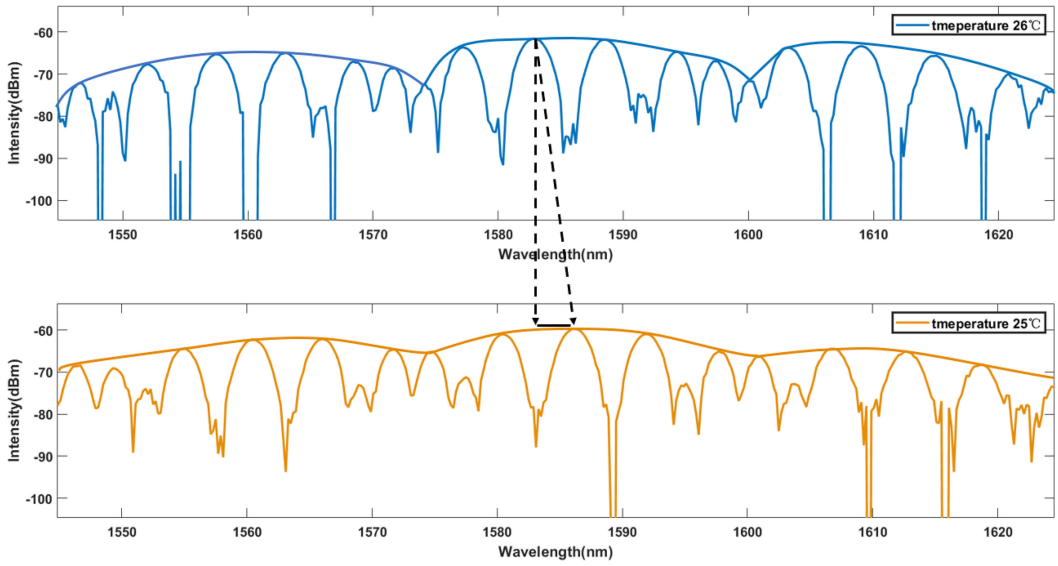

Fig. 5. The transmission spectrum shifts of cascaded Sagnac interferometer.

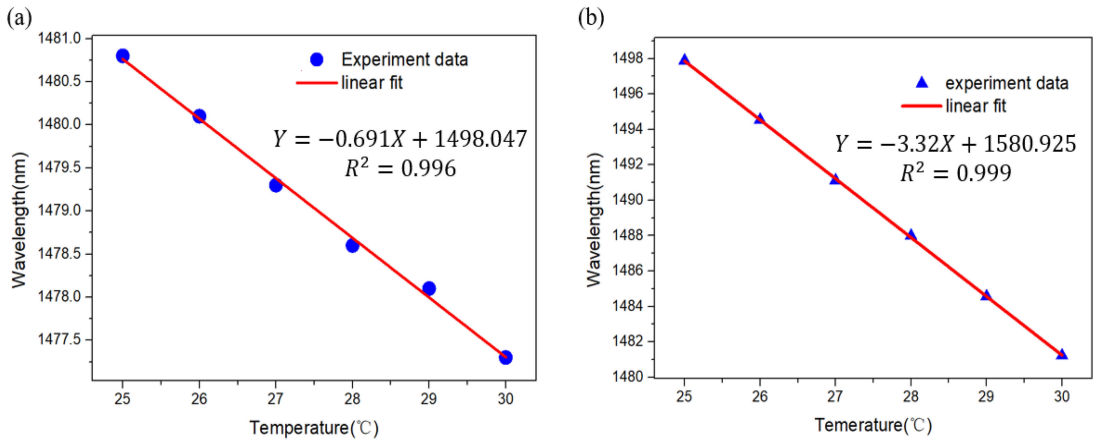

Fig. 6. Linear fitting and error bars of the relationship between temperature and wavelength shift. (from 20 °C-32 °C) (a) single Sagnac loop and (b)cascaded Sagnac loops.

structure sensor is compared. Compared with the temperature sensitivity of a single Sagnac loop (-0.69 nm / °C), the temperature sensitivity of cascaded Sagnac loop is improved (- 3.32 nm / °C). The R^2 of the sensor head is ∼0.999 and ∼0.996, respectively. Owing to the uncertainty measurement error of the envelope position in the spectrum. The final magnification of the experiment is ∼4.81, slightly larger than the theoretical value (∼4.54). Considering computed enhancement factor (see (11)), the sensitivity can be effectively increased by selecting two interferometers with small difference in FSR. However, in practical applications, there is a tread off between the sensitivity and measurement accuracy. Smaller difference in FSR will increase the envelope. Thus, the number of envelopes within the determined wavelength range is reduced. Therefore, it is difficult to track the offset of the envelope peak. Hence, a FRL temperature sensor based on cascaded Sagnac loops is proposed, which can effectively reduce the detection error caused by the shift of the tracking envelope peak through reading the spectral shift directly.

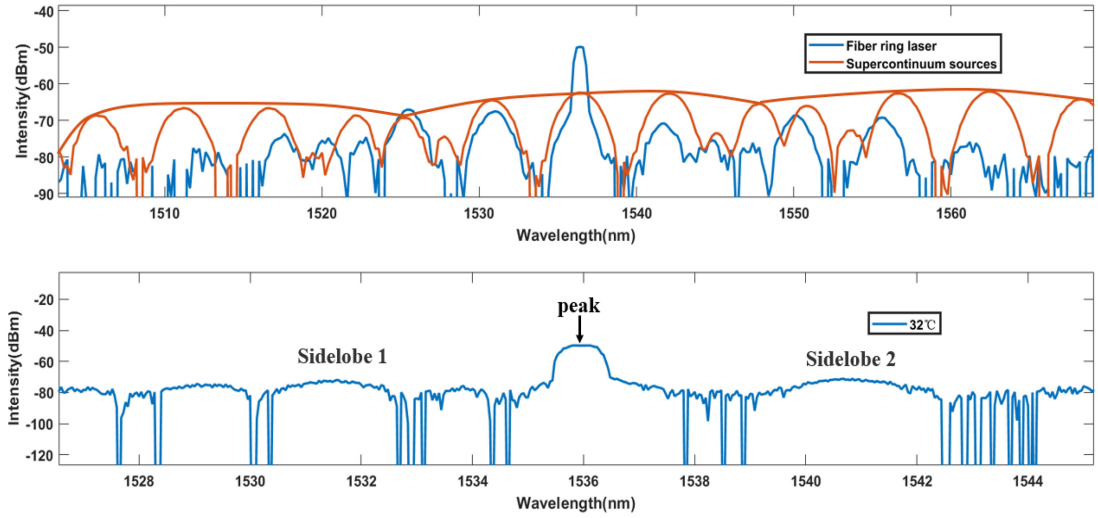

Fig. 7. The transmission spectrum of Sagnac loop and output of the SLED sensor at 24 °C (purple color). (b) The transmission spectrum of the Sagnac loop and output of the fiber laser sensor at 33 °C.

4. Results

The measured spectra showed multiple envelopes in the C+L band as shown in Fig. 7. However, we found that the single-wavelength laser could oscillate in the main lobe at a certain range. Hence, we found that in order to realize the accurate measurement of the temperature sensor, the dry bath temperature should be controlled in the range of 25 °C to 31 °C. When the temperature exceeds this range, since the erbium-doped fiber concentrated in the C + L band, the frequency hopping will occur. As shown in Fig. 7, when the temperature is 24 °C and 32 °C, the output laser wavelength overlaps at 1536 nm. Besides, the side lobe can also provide energy for the corresponding wavelength in the process of laser building-up. Therefore, the laser spectrum will be similar to that of cascaded Sagnac rings in SLED. The main lobe begins to get energy to produce the laser, and the side lobe also gets part of the energy. This may be the reason why the spectrum of the sensor is wider than that of the ordinary FRL sensor. Fig. 7 depicts the measured output spectra of the cascaded Sagnac fiber ring structure in the scanning wavelength range of 1500 nm to 1580 nm: broadband light source (orange Line) and fiber ring laser (blue line). The peak wavelength of cascade Sagnac ring structure in FRL is consistent with that in broadband light source. It is worth noting that the fiber ring laser sensor has high SNR and narrow 3dB bandwidth. The SNR of the proposed FRL sensing system is more than ∼30dB, which is 3-5 times larger than that of the traditional sensing system. Besides, the 3dB bandwidth (∼0.67 nm) is much smaller than the traditional sensing system (∼10 nm).

The output spectra of the sensing system are measured in Fig. 8 and Fig. 9 with the temperature controlled from 26 °C to 32 °C. The peak wavelength was shifted to a shorter wavelength accordingly. (i.e., the laser wavelength has a blue-shift with the increase of temperature). Moreover, With the change of temperature, the birefringence of PMF in Sagnac loop changes, and the transmission spectrum of Sagnac loop shifts to a shorter wavelength. Besides, the response of the single Sagnac loop structure to temperature variations has also been analyzed. The FRL sensor based on individual Sagnac loop is placed into a temperature-controlled dry bath. The wavelength shift varies with ambient temperature from 25 °C to 31 °C, as shown in Fig. 8.

Fig. 10(a) and Fig. 10(b) show the lasing wavelength as a function of the temperature. When temperature is varied from 25 °C to 31 °C, the linear fitting is 0.998 and 0.999, respectively. The result proves that the relationship between the wavelength of laser and temperature is linear. Besides, the peak intensity of the laser is shown in Fig. 11. where the peak intensity is between

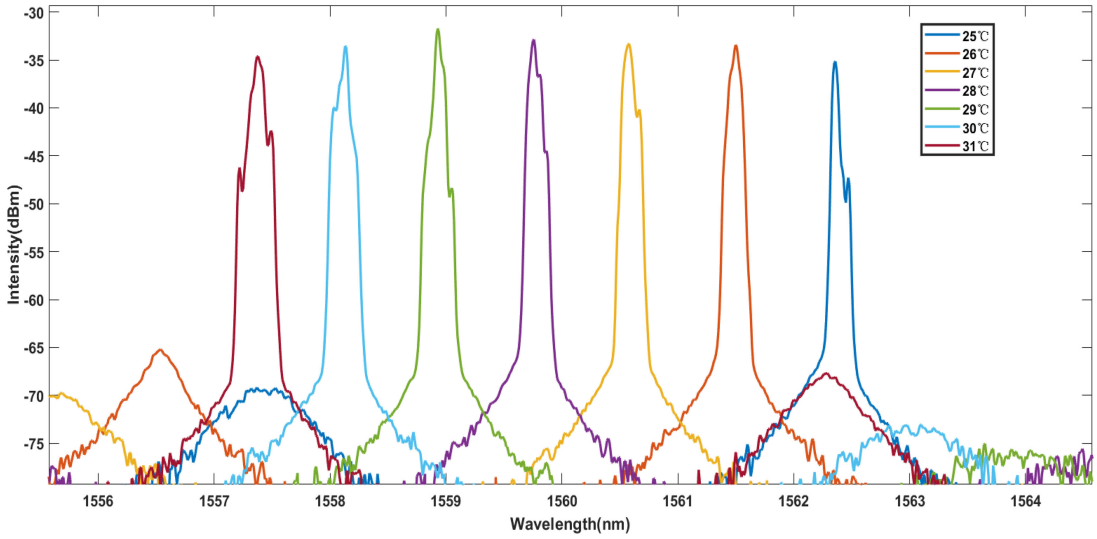

Fig. 8. Transmission spectra of the fiber laser temperature sensor based on single Sagnac loop system when T changes from 25 °C to 31 °C with the steps of 1 °C.

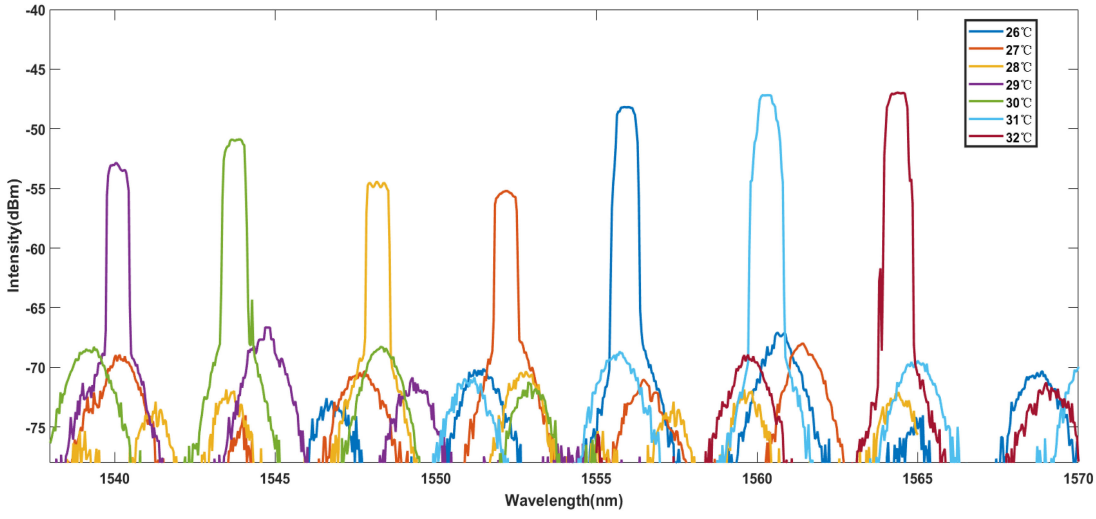

Fig. 9. Transmission spectra of the fiber laser temperature sensor based on cascaded Sagnac loops system when T changes from 25 °C to 31 °C with the steps of 1 °C.

−47.12 dBm and −48.22 dBm. The wavelength fluctuation range is 1560.37 nm to 1561.23 nm at 3 hours which shows that the proposed laser sensor system in this work is highly stable after long-time of work. The central wavelength shifts from 1564.41 nm to 1540.22 nm when the temperature changes from 25 °C to 31 °C, corresponding to a temperature sensitivity of ∼-4.03 nm/ °C and the level of temperature resolution is 10^{-3} °C. According to Fig. 10 (a), the corresponding temperature sensitivity of a single Sagnac ring temperature sensor is ∼-0.826 nm/ °C. Therefore, the experimental enhancement factor is ∼4.879, which is similar to the previous amplification factor (4.81). Moreover, better results can be obtained by choosing the length of erbium-doped fiber properly. The spectral broadening of cascaded Sagnac structure relative to single Sagnac loop structure may be caused by the change of the free spectral range which was described in [37].

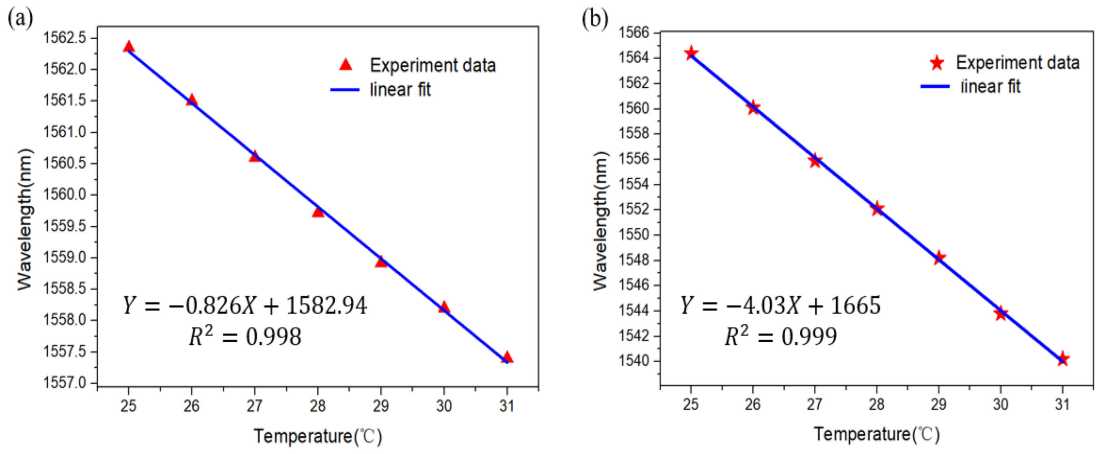

Fig. 10. Linear fitting and error bars of the relationship between temperature and wavelength shift. (from 20 °C-32 °C))a(Single Sagnac loop sensing system and (b) Cascaded Sagnac loops sensing system.

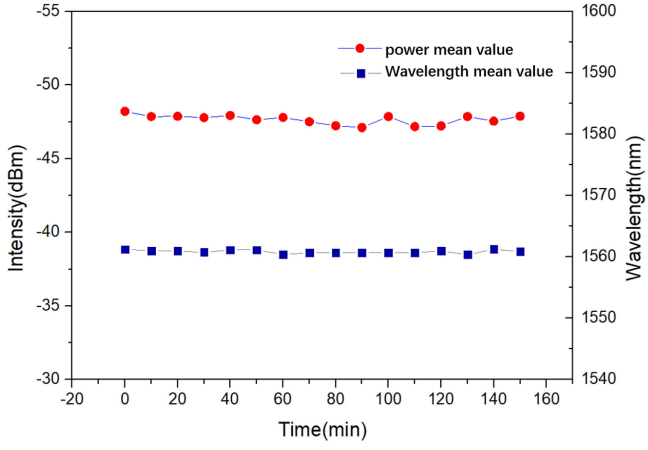

Fig. 11. Test for time stability of wavelength shift and power fluctuation.

TABLE 1
Comparison Between the Proposed Sensor and References

Ref.	Structure of sensing head	Sensitivity(nm/℃)	Measurement range(℃)	Linearity(R^2)
[24]	liquid filled PCF	-1.747	25-31	0.999
[25]	core-offset Mach-Zehnder	0.049	22-50	No Given
[26]	Fabry–Perot Interferometer	0.249	33-55	0.993
[30]	individual Sagnac loop	-1.728	30-40	0.986
[38]	single-mode-tapered cladding less-single-mode	0.011	8-80	0.992
This work	cascaded Sagnac loops	-4.031	25-31	0.999

Table 1 shows the performance comparison (sensitivity, measurement range and linearity) of the FRL temperature sensors based on different kinds of structure. To the best of our knowledge, our sensor shows the best sensitivity performance. The sensor is composed of cascaded Sagnac loop with uniform polarization maintaining fiber based on the Vernier effect. Furthermore, it has the characteristics of high temperature sensitivity and remote temperature detection by extending the length of Sagnac ring. Moreover, it has broad application prospects in the field of environmental monitoring.

5. Conclusion

In summary, an ultra-high sensitivity FRL temperature sensor based on cascaded Sagnac loops structure is proposed and experimentally demonstrated. PMF lengths of 56 cm and 75 cm were selected to construct Sagnac loop. Moreover, the cascaded loops work as a filter and the sensing unit inside the fiber laser ring cavity. The sensitivity of the sensor is improved by Vernier effect. In conclusion, an ultra-high temperature sensitivity of ∼-4.031 nm/ °C is realized. The results show that the system can significantly improve the sensing performance by ∼4.879 times. Finally, the sensitivity is increased to 4.54 times by theoretical calculation, which is very close to the experimental results. The error may be due to the inaccurate selection of envelope. This technique could be explored to measure harsh environment.

References

[1] X. Zou, M. Li, W. Pan, L. Yan, and L. Shao, "Multichannel narrow, flat-top optical filters based on multiple-phase-shifted and phase sampled FBG," *IEEE J. Quantum Electron.*, vol. 53, no. 1, pp. 1–5, Feb. 2017.

[2] L. Jin *et al.*, "An embedded FBG sensor for simultaneous measurement of stress and temperature," *IEEE Photon. Technol. Lett.*, vol. 18, no. 1, pp. 154–156, Jan. 2006.

[3] T. Guo, F. Liu, B.-O. Guan, and J. Albert, "Tilted fiber grating mechanical and biochemical sensors," *Opt. Laser Technol.*, vol. 78, pp. 19–33, 2016.

[4] J. Hu *et al.*, "Dual mach–zehnder interferometer based on side-hole fiber for high-sensitivity refractive index sensing," *IEEE Photon. J.*, vol. 11, no. 6, pp. 1–13, Dec. 2019.

[5] W. Ni *et al.*, "Single hole twin eccentric core fiber sensor based on anti-resonant effect combined with inline Mach-Zehnder interferometer," *Opt. Exp.*, vol. 25, no. 11, pp. 12372–12380, May 2017.

[6] S. Marrujo-Garcia, I. Hernandez-Romano, M. Torres-Cisneros, D. A. May-Arrioja, V. P. Minkovich, and D. Monzon-Hernandez, "Temperature-independent curvature sensor based on in-fiber Mach-Zehnder interferometer using hollow-core fiber," *J. Lightw. Technol.*, vol. 38, no. 15, pp. 4166–4173, Aug. 2020.

[7] Y. Liu *et al.*, "Hollow-core fiber-based all-fiber FPI sensor for simultaneous measurement of air pressure and temperature," *IEEE Sensors J.*, vol. 19, no. 23, pp. 11236–11241, Dec. 2019.

[8] A. Zhou *et al.*, "Hybrid structured fiber-optic Fabry-Perot interferometer for simultaneous measurement of strain and temperature," *Opt. Lett*, vol. 39, no. 18, pp. 5267–5270, Sep 2014.

[9] Y. Liu and S. Qu, "Optical fiber Fabry-Perot interferometer cavity fabricated by femtosecond laser-induced water breakdown for refractive index sensing," *Appl. Opt.*, vol. 53, no. 3, pp. 469–474, Jan. 2014.

[10] L.-Y. Shao *et al.*, "High-frequency ultrasonic hydrophone based on a cladding-etched DBR fiber laser," *IEEE Photon. Technol. Lett.*, vol. 20, no. 8, pp. 548–550, Apr. 2008.

[11] X. Yang, S. Bandyopadhyay, L.-Y. Shao, D. Xiao, G. Gu, and Z. Song, "Side-polished DBR fiber laser with enhanced sensitivity for axial force and refractive index measurement," *IEEE Photon. J.*, vol. 11, no. 3, pp. 1–10, Jun. 2019.

[12] H. Ishii, F. Kano, Y. Tohmori, Y. Kondo, T. Tamamura, and Y. Yoshikuni, "Narrow spectral linewidth under wavelength tuning in thermally tunable super-structure-grating (SSG) DBR lasers," *IEEE J. Sel. Topics Quantum Electron.*, vol. 1, no. 2, pp. 401–407, Jun. 1995.

[13] J. M. Tang and K. A. Shore, "30-gb/s signal transmission over 40-km directly modulated DFB-laser-based single-mode-fiber links without optical amplification and dispersion compensation," *J. Lightw. Technol.*, vol. 24, no. 6, pp. 2318–2327, 2006.

[14] D. Leandro, V. deMiguel Soto, R. A. Perez-Herrera, M. Bravo Acha, and M. Lopez-Amo, "Random DFB fiber laser for remote (200 km) sensor monitoring using hybrid WDM/TDM," *J. Lightw. Technol.*, vol. 34, no. 19, pp. 4430–4436, 2016.

[15] W. Fan, B. Chen, X. Li, L. Chen, and Z. Lin, "Stress-induced single polarization DFB fiber lasers," *Opt. Commun.*, vol. 204, no. 1-6, pp. 157–161, 2002.

[16] K. Tamura, E. P. Ippen, H. A. Haus, and L. E. Nelson, "77-fs pulse generation from a stretched-pulse mode-locked all-fiber ring laser," *Opt. Lett*, vol. 18, no. 13, pp. 1080, Jul 1 1993.

[17] J. Shi *et al.*, "Remote Gas Pressure Sensor Based on Fiber Ring Laser Embedded With Fabry–Pérot Interferometer and Sagnac Loop," *IEEE Photon. J.*, vol. 8, no. 5, pp. 1–8, Oct. 2016.

[18] L.-Y. Shao, J. Liang, X. Zhang, W. Pan, and L. Yan, "High resolution refractive index sensing with dual-wavelength fiber laser," *IEEE Sensors J.*, vol. 16, no. 23, pp. 8463–8467, Dec. 2016.

[19] Z.-B. Liu, Y. Li, Y. Liu, Z.-W. Tan, and S. Jian, "A static axial strain fiber ring cavity laser sensor based on multi-modal interference," *IEEE Photon. Technol. Lett.*, vol. 25, no. 21, pp. 2050–2053, Nov. 2013.

[20] L. Shen *et al.*, "Distributed curvature sensing based on a bending loss-resistant ring-core fiber," *Photonics*, vol. 8, no. 2, pp. 165–174, 2020.

[21] M. Bosch, A. Sánchez, F. Rojas, and C. Ojeda, "Recent development in optical fiber biosensors," *Sensors*, vol. 7, no. 6, pp. 797–859, 2007.

[22] P. Antunes, H. Lima, H. Varum, and P. André, "Optical fiber sensors for static and dynamic health monitoring of civil engineering infrastructures: Abode wall case study," *Measurement*, vol. 45, no. 7, pp. 1695–1705, 2012.

[23] C. A. F. Marques, A. Pospori, D. Saez-Rodriguez, K. Nielsen, O. Bang, and D. J. Webb, "Aviation fuel gauging sensor utilizing multiple diaphragm sensors incorporating polymer optical fiber bragg gratings," *IEEE Sensors J.*, vol. 16, no. 15, pp. 6122–6129, Aug. 2016.

[24] X. C. Yang, Y. Lu, B. L. Liu, and J. Q. Yao, "Fiber ring laser temperature sensor based on liquid-filled photonic crystal fiber," *IEEE Sensors J.*, vol. 17, no. 21, pp. 6948–6952, Nov. 2017.
[25] L. Cai, Y. Zhao, and X. G. Li, "A fiber ring cavity laser sensor for refractive index and temperature measurement with core-offset modal interferometer as tunable filter," *Sensors Actuators B: Chem.*, vol. 242, pp. 673–678, 2017.
[26] H. Zou, L. Ma, H. Xiong, Y. Zhang, and Y. T. Li, "Fiber ring laser sensor based on Fabry–Perot cavity interferometer for temperature sensing," *Laser Phys.*, vol. 28, no. 1, 2018.
[27] Q. Zhao *et al.*, "Tunable and interval-adjustable multi-wavelength erbium-doped fiber laser based on cascaded filters with the assistance of NPR," *Opt. Laser Technol.*, vol. 131, 2020.
[28] Y. Chang, L. Pei, T. Ning, J. Zheng, J. Li, and C. Xie, "Switchable and tunable multi-wavelength fiber ring laser employing a cascaded fiber filter," *Opt. Fiber Technol.*, vol. 58, 2020.
[29] S. Feng, O. Xu, S. Lu, X. Mao, T. Ning, and S. Jian, "Switchable dual-wavelength erbium-doped fiber-ring laser based on one polarization maintaining fiber Bragg grating in a Sagnac loop interferometer," *Opt. Laser Technol.*, vol. 41, no. 3, pp. 264–267, 2009.
[30] J. Shi *et al.*, "Temperature sensor based on fiber ring laser with sagnac loop," *IEEE Photon. Technol. Lett.*, vol. 28, no. 7, pp. 794–797, Apr. 2016.
[31] J. Shi *et al.*, "High-resolution temperature sensor based on intracavity sensing of fiber ring laser," *J. Lightw. Technol.*, vol. 38, no. 7, pp. 2010–2014, 2020.
[32] C. S. Kim, F. N. Farokhrooz, and J. U. Kang, "Electro-optic wavelength-tunable fiber ring laser based on cascaded composite Sagnac loop filters," *Opt. Lett*, vol. 29, no. 14, pp. 1677–1679, Jul. 2004.
[33] L. Ma, Z. Kang, Y. Qi, and S. Jian, "Tunable dual-wavelength fiber laser based on an MMI filter in a cascaded Sagnac loop interferometer," *Laser Phys.*, vol. 24, no. 4, 2014.
[34] Y. Li, Q. Sun, Z. Xu, Y. Luo, and D. Liu, "A single longitudinal mode fiber ring laser based on cascaded microfiber knots filter," *IEEE Photon. Technol. Lett.*, vol. 28, no. 20, pp. 2172–2175, Oct. 2016.
[35] L.-Y. Shao *et al.*, "Sensitivity-enhanced temperature sensor with cascaded fiber optic Sagnac interferometers based on Vernier-effect," *Opt. Commun.*, vol. 336, pp. 73–76, 2015.
[36] H. Zou, S. Lou, G. Yin, and W. Su, "Switchable dual-wavelength PM-EDF ring laser based on a novel filter," *IEEE Photon. Technol. Lett.*, vol. 25, no. 11, pp. 1003–1006, Jun. 2013.
[37] M. Pollnau and M. Eichhorn, "Spectral coherence, Part I: Passive-resonator linewidth, fundamental laser linewidth, and Schawlow-Townes approximation," *Prog. Quantum Electron.*, vol. 72, 2020.
[38] L. Linjun, R. Guobin, Y. Bin, P. Wanjin, L. Xiao, and J. Shuisheng, "Refractive index and temperature sensor based on fiber ring laser with STCS fiber structure," *IEEE Photon. Technol. Lett.*, vol. 26, no. 21, pp. 2201–2204, Nov. 2014.